



Suppression of bending waves in a beam using a tuned vibration absorber

H.M. El-Khatib*, B.R. Mace, M.J. Brennan

Research: Dynamics Group, Institute of Sound and Vibration Research, University of Southampton, Highfield, Southampton SO17 1BJ, UK

Received 15 March 2004; received in revised form 7 October 2004; accepted 26 January 2005
Available online 7 April 2005

Abstract

This paper is concerned with the control of flexural waves in a beam using a tuned vibration absorber (TVA). The TVA may be located in the farfield or the nearfield of a time harmonic point force and it can be positioned to control both the downstream-transmitted power and that reflected upstream. Analytical and numerical investigations are presented. The effects of the incident evanescent wave on the optimal characteristics of the absorber are discussed when the TVA is located in the nearfield of the point force.

If the TVA is located in the nearfield, the power transmitted past the TVA depends on four independent tuning parameters: the absorber frequency, the mass ratio, the structural damping of the TVA and the distance between the TVA and the point force. If the incident nearfield wave is insignificant, then this distance becomes unimportant in determining the optimal characteristics of the TVA. The net power propagating upstream is due to the superposition of the wave reflected from the TVA and that input by the point force and depends on all four parameters.

Attention is focussed on finding the frequencies at which the minimum power is transmitted or the maximum power absorbed by the TVA. Experimental results are presented to validate the theoretical predictions.

© 2005 Elsevier Ltd. All rights reserved.

*Corresponding author. Tel.: +44 23 8059 2276; fax: +44 23 8059 3190.
E-mail address: hek@isvr.soton.ac.uk (H.M. El-Khatib).

tuned frequency. The cases of optimal energy absorption by the device or minimisation of the transmission of a propagating wave are considered. The presence of an incident evanescent wave, together with the incident propagating wave, affects the optimal characteristics of the TVA. The net upstream propagating wave is also considered. This is given by the superposition of the wave reflected by the TVA and the upstream wave generated by the point force, and depends on the location of the TVA together with its parameters.

The paper is set out as follows. Section 2 concerns the dynamic behaviour of the TVA and the way in which it affects wave transmission. The reflection and transmission matrices are found. The power transmitted downstream of the TVA is found in terms of four independent parameters: the ratio of the tuned frequency to the TVA frequency, the loss factor of the TVA, the mass of the TVA and the distance between the TVA and the source of disturbance. The maximum power that can be absorbed by the TVA is investigated as well as the optimum tuning parameters of the absorber. Section 3 is devoted to numerical examples, investigating the performance of the TVA and the optimum tuning parameters of the absorber for both nearfield and farfield cases. The TVA can be optimised either for minimum transmission or maximum energy absorption. Experimental validation of the theoretical predictions is reported in Section 4. Finally, conclusions are presented.

2. Dynamic behaviour of a TVA on a beam

The aim of this section is to investigate the reflection and transmission of waves at a TVA on a beam when the TVA is in either the nearfield or the farfield of a point force disturbance.

2.1. Reflection and transmission coefficients

Consider the TVA modelled as a single degree of freedom (SDOF) system and mounted on a beam at $x = 0$ and at a distance l from an applied force $F \exp(i\omega t)$ as shown in Fig. 1. Here m_a , k_a and η are the mass, stiffness and the loss factor of the TVA, respectively. The force generates

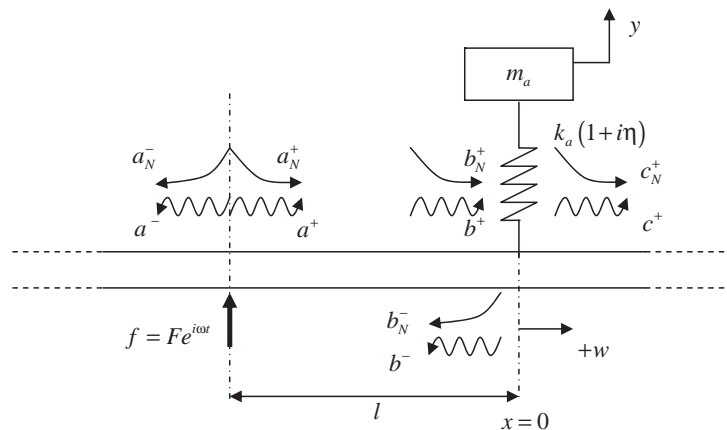


Fig. 1. TVA in nearfield of point force.

waves, which are incident on the TVA and are partly reflected and partly transmitted. The ratios of the reflected and transmitted wave amplitudes to those of the incident waves depend on the characteristics of the TVA. The wave components shown in Fig. 1 represents positive- and negative-going propagating waves generated by the point force (a^+, a^-), positive- and negative-going propagating waves at a distance l from the point force (b^+, b^-) and the transmitted propagating wave (c^+). The amplitudes a, b and c are complex; the subscript N refers to evanescent waves. The net upstream propagating wave ($a^- + b^-e^{-ikl}$) is the superposition of the wave reflected from the TVA and the upstream wave generated by the point force.

Suppressing the $e^{i\omega t}$ time dependence for clarity, the beam displacement is given by

$$w_+ = c^+e^{-ikx} + c_N^+e^{-kx}; \quad w_- = b^+e^{-ikx} + b_N^+e^{-kx} + b^-e^{ikx} + b_N^-e^{kx}, \tag{1}$$

where w_+ and w_- are the displacements of the beam in the regions $x \geq 0$ and $-l \leq x \leq 0$, respectively. A list of symbols is given in Nomenclature. Here, $k = \sqrt[4]{\rho A/EI} \sqrt{\omega}$ is the flexural wavenumber of the beam and ρ, A and EI are the density, cross-sectional area and flexural rigidity of the beam, respectively.

The force generates waves of amplitudes [8,9]

$$\begin{Bmatrix} a^+ \\ a_N^+ \end{Bmatrix} = \frac{-F}{4EI k^3} \begin{Bmatrix} i \\ 1 \end{Bmatrix}, \tag{2}$$

the waves incident on the TVA are

$$\begin{Bmatrix} b^+ \\ b_N^+ \end{Bmatrix} = \begin{bmatrix} e^{-ikl} & 0 \\ 0 & e^{-kl} \end{bmatrix} \begin{Bmatrix} a^+ \\ a_N^+ \end{Bmatrix}, \tag{3}$$

while the amplitudes of the reflected and transmitted waves are given by

$$\begin{Bmatrix} b^- \\ b_N^- \end{Bmatrix} = \mathbf{r} \begin{Bmatrix} b^+ \\ b_N^+ \end{Bmatrix},$$

$$\begin{Bmatrix} c^+ \\ c_N^+ \end{Bmatrix} = \mathbf{t} \begin{Bmatrix} b^+ \\ b_N^+ \end{Bmatrix}. \tag{4a,b}$$

Here \mathbf{r} and \mathbf{t} are the reflection and transmission matrices for the TVA.

The reflection and transmission matrices can be found by considering the continuity and equilibrium conditions. Continuity of displacement ($w_+(0) = w_-(0)$) gives, from Eq. (1)

$$c^+ + c_N^+ = b^+ + b_N^+ + b^- + b_N^-. \tag{5}$$

Continuity of rotation ($\partial w_+(0)/\partial x = \partial w_-(0)/\partial x$) gives

$$-ic^+ - c_N^+ = -ib^+ - b_N^+ + ib^- + b_N^-. \tag{6}$$

From equilibrium of shear forces

$$ic^+ - c_N^+ - ib^+ + b_N^+ + ib^- - b_N^- = \frac{k_a}{EI k^3} (1 + i\eta)(y - w(0)). \tag{7}$$

The term on the right is force on the beam from the absorber, whose mass has a displacement y .

Equilibrium of bending moments gives

$$-c^+ + c_N^+ = -b^+ + b_N^+ - b^- + b_N^- \tag{8}$$

Finally, the displacement of the absorber’s mass is given by

$$y = \left(\frac{k_a(1 + i\eta)}{k_a(1 + i\eta) - m_a\omega^2} \right) w(0). \tag{9}$$

Eqs. (1), (5)–(8) and (9) can be solved for the reflection and transmission matrices **r** and **t**, which are

$$\mathbf{r} = \beta \begin{bmatrix} i & i \\ 1 & 1 \end{bmatrix}, \quad \mathbf{t} = \mathbf{I} + \mathbf{r}, \tag{10a,b}$$

where **I** is the identity matrix and

$$\beta = \frac{\gamma\Omega^{1/2}(1 + i\eta)}{\Omega^2 - (1 + i\eta)(1 + \gamma\Omega^{1/2}(1 + i))}, \tag{11}$$

The dimensionless parameters

$$\gamma = \frac{\pi m_a}{2\rho A\lambda_a}, \quad \Omega = \frac{\omega}{\omega_a}, \tag{12a,b}$$

represent, respectively, the mass ratio γ at the absorber frequency $\omega_a = \sqrt{k_a/m_a}$, i.e. the ratio of the mass of the absorber to the mass in a length $2\lambda_a/\pi$ of the beam (where λ_a is the wavelength at ω_a) and the frequency ratio Ω , which is the ratio of the excitation frequency ω to the absorber frequency ω_a . The variable kl that appears in Eq. (3) can be re-written in terms of the non-dimensional parameters as

$$kl = 2\pi\sqrt{\Omega} \left(\frac{l}{\lambda_a} \right). \tag{13}$$

2.2. Transmitted power

The transmitted propagating wave c^+ , which carries energy to the farfield downstream of the TVA, has components arising from both the propagating and nearfield incident waves b^+ and b_N^+ . It is given by

$$c^+ = \frac{-iFe^{-ikl}}{4EI k^3} \left[\frac{\Omega^2 - (1 + i\eta)(1 + \gamma\Omega^{1/2}(1 - e^{-kl(1-i)}))}{\Omega^2 - (1 + i\eta)(1 + \gamma\Omega^{1/2}(1 + i))} \right]. \tag{14}$$

It can be seen that c^+ depends on the location of the TVA with respect to the disturbance through the terms involving kl .

The transmission ratio τ_t of the absorber is now defined as the ratio of the power transmitted to that which would be transmitted if the absorber were absent, i.e. $\tau_t = |c^+/a^+|^2$

and is given by

$$\tau_t = \left| \frac{\Omega^2 - (1 + i\eta)(1 + \gamma\Omega^{1/2}(1 - e^{-kl(1-i)}))}{\Omega^2 - (1 + i\eta)(1 + \gamma\Omega^{1/2}(1 + i))} \right|^2. \quad (15)$$

Therefore, the transmitted power also depends on the distance l .

If the TVA is attached at the source of disturbance, then $l = 0$ and the transmission ratio becomes

$$\tau_t = \left| \frac{\Omega^2 - (1 + i\eta)}{\Omega^2 - (1 + i\eta)(1 + \gamma\Omega^{1/2}(1 + i))} \right|^2. \quad (16)$$

If the TVA is attached in the farfield of the disturbance, then kl is large and the transmitted power becomes

$$\tau_t = \left| \frac{\Omega^2 - (1 + i\eta)(1 + \gamma\Omega^{1/2})}{\Omega^2 - (1 + i\eta)(1 + \gamma\Omega^{1/2}(1 + i))} \right|^2. \quad (17)$$

The transmission ratio depends on the absorber parameters and the frequency ratio in a somewhat complicated manner.

2.3. Upstream power

The net wave propagating upstream of the point force ($a^- + b^-e^{-ikl}$) is given by

$$(a^- + b^-e^{-ikl}) = \frac{-iF}{4EIk^3} \left[1 + ie^{-2ikl} \left[\frac{\gamma\Omega^{1/2}(1 + i\eta)(1 - ie^{-kl(1-i)})}{\Omega^2 - (1 + i\eta)(1 + \gamma\Omega^{1/2}(1 + i))} \right] \right]. \quad (18)$$

The reflection ratio τ_r is defined as the ratio of the power reflected upstream to that which would propagate upstream if the absorber were absent, i.e. $\tau_r = |(a^- + b^-e^{-ikl})/a^-|^2$ and is given by

$$\tau_r = \left| 1 + ie^{-2ikl} \left[\frac{\gamma\Omega^{1/2}(1 + i\eta)(1 - ie^{-kl(1-i)})}{\Omega^2 - (1 + i\eta)(1 + \gamma\Omega^{1/2}(1 + i))} \right] \right|^2. \quad (19)$$

If the TVA is attached at the source of disturbance then the reflection ratio is equal to the transmission ratio given by Eq. (16), while if the TVA is attached in the farfield of the disturbance, then τ_r reduces to

$$\tau_r = \left| 1 + ie^{-2ikl} \left[\frac{\gamma\Omega^{1/2}(1 + i\eta)}{\Omega^2 - (1 + i\eta)(1 + \gamma\Omega^{1/2}(1 + i))} \right] \right|^2. \quad (20)$$

2.4. Optimum tuning of the TVA

In this section some comments are made concerning the optimum tuning parameters of the TVA. It is possible to either minimise the power transmitted both downstream and upstream or to maximise the power absorbed by the TVA. In the first case ideally $\eta = 0$ while in the second case

there is an optimum value of structural damping in the TVA. If the incident evanescent wave is significant, then the distance l between the force and the position of the TVA also affects the optimum tuning parameters.

In general, numerical solutions are required to determine the optimum tuning parameters. However, for the case of an undamped TVA, analytical expressions exist for various special cases and some are given in this section, together with certain approximations valid for small values of the absorber parameters.

If the TVA is undamped $\eta = 0$ and the transmission and reflection ratios become

$$\tau_t = \left| \frac{\Omega^2 - (1 + \gamma\Omega^{1/2}(1 - e^{-kl(1-i)}))}{\Omega^2 - (1 + \gamma\Omega^{1/2}(1 + i))} \right|^2,$$

$$\tau_r = \left| 1 + ie^{-2ikl} \left[\frac{\gamma\Omega^{1/2}(1 - ie^{-kl(1-i)})}{\Omega^2 - (1 + \gamma\Omega^{1/2}(1 + i))} \right] \right|^2. \tag{21a,b}$$

The tuned frequency Ω_t is now defined to be the frequency ratio at which the transmitted power is minimum. If the TVA is attached to the source of disturbance (i.e. $kl = 0$), then $\Omega_t = 1$, so that minimum transmission occurs at the absorber frequency, where the impedance of the absorber is infinite. At this frequency the transmission and reflection ratios are both zero.

If the TVA is located in the farfield (i.e. $kl \rightarrow \infty$), then the tuned frequency ratio satisfies

$$\Omega_t^2 - \gamma\Omega_t^{1/2} - 1 = 0. \tag{22}$$

Increasing the mass ratio increases Ω_t . At this frequency the transmitted power is zero. There is no analytical solution for Ω_t , but approximate solutions can be found for small and large γ , namely

$$\begin{aligned} \Omega_t &\approx 1 + \gamma/2, & \gamma \ll 1, \\ \Omega_t &\approx \gamma^{2/3}, & \gamma \gg 1. \end{aligned} \tag{23a,b}$$

This case is discussed in detail in [3].

In the general case Ω_t depends on the TVA location l and the minimum transmission ratio is not zero. A numerical solution can be found by minimising τ_t . For small γ this yields

$$\Omega_t \approx 1 + \frac{\gamma}{2}(1 - e^{-kl} \cos kl), \tag{24}$$

while if $kl \ll 1$

$$\Omega_t \approx 1 + \frac{\gamma kl}{2}. \tag{25}$$

In this latter case the minimum transmitted power is approximately $\tau_{t,\min} \approx (kl)^2/2$. The small and large kl asymptotes of Eqs. (23a) and (25) intersect when $kl = 1$.

The maximum transmission ratio is greater than 1 and occurs at a frequency ratio $\Omega_m > \Omega_t$ which also depends on the TVA location. If the TVA is attached at the disturbance location then

$$\Omega_m^2 - 2\gamma\Omega_m^{1/2} - 1 = 0 \tag{26}$$

and the maximum power transmitted is $\tau_{t,\max} = 2$. For small γ , $\Omega_m \approx 1 + \gamma$. Hence increasing the mass ratio increases the frequency ratio Ω_m at which the maximum transmission occurs. The maximum transmission occurs due to matching of the impedance of the undamped absorber to the reactive part of the impedance of the beam at this frequency. The maximum power transmitted decreases as kl increases, becoming equal to 1 as $kl \rightarrow \infty$.

The net wave propagating upstream for a TVA attached in the farfield can be written as

$$(a^- + b^- e^{-ikl}) = a^-(1 + |r_{11}|e^{-i(2kl+\phi)}), \quad (27)$$

where $|r_{11}|$ and ϕ are the magnitude and phase of the (1,1) element of the reflection matrix. If the absorber is undamped and optimally tuned, then the transmission coefficient $t_{11} = 0$ and the reflection coefficient $r_{11} = -1$. Therefore Eq. (27) becomes

$$(a^- + b^- e^{-ikl}) = a^-(1 - e^{-i2kl}). \quad (28)$$

If the total phase shift $2kl = (2n - 1)\pi$, where n is any integer, then the amplitude of the upstream wave in the farfield is $2a^-$: the reflected wave interferes constructively with the upstream wave injected by the disturbance. On the other hand, if $2kl = 2n\pi$, then the amplitude of the upstream-going wave is zero: the two wave components interfere destructively. Thus the location l of the undamped absorber can be chosen in order to obtain zero transmission upstream if the absorber is located in the farfield. It can be seen therefore, that the transmitted and reflected power can be completely suppressed at a single frequency using a single undamped TVA located in the correct position in the farfield.

If the TVA is not in the farfield then the phase of r_{11} is somewhat different from $-\pi$, while its magnitude is somewhat less than 1, so that total cancellation of the upstream going wave does not occur.

3. Numerical examples

The dependence of the power transmitted and absorbed on the TVA parameters is illustrated numerically in this section.

3.1. Effect of TVA location

Fig. 2 shows the transmission ratio τ_t as a function of the frequency ratio Ω for two different mass ratios γ and various locations of the TVA, l/λ_a , where $\lambda_a = 2\pi/k$ is the bending wavelength at the absorber frequency. The TVA is assumed to be undamped. Generally, in each case the transmission has a minimum at a certain frequency Ω_t . However, in all cases $\Omega_t = 1$ when $l = 0$ and the transmission ratio asymptotes to 1 as $\Omega \rightarrow \infty$. It can be seen that $\tau_t > 1$ for some $\Omega > \Omega_t$ and increasing l/λ_a reduces the maximum transmission ratio. Also, increasing l/λ_a increases the tuned frequency. When the nearfield wave is significant, the transmission ratio of the undamped absorber is no longer zero at Ω_t . Moreover, increasing the mass ratio increases Ω_t .

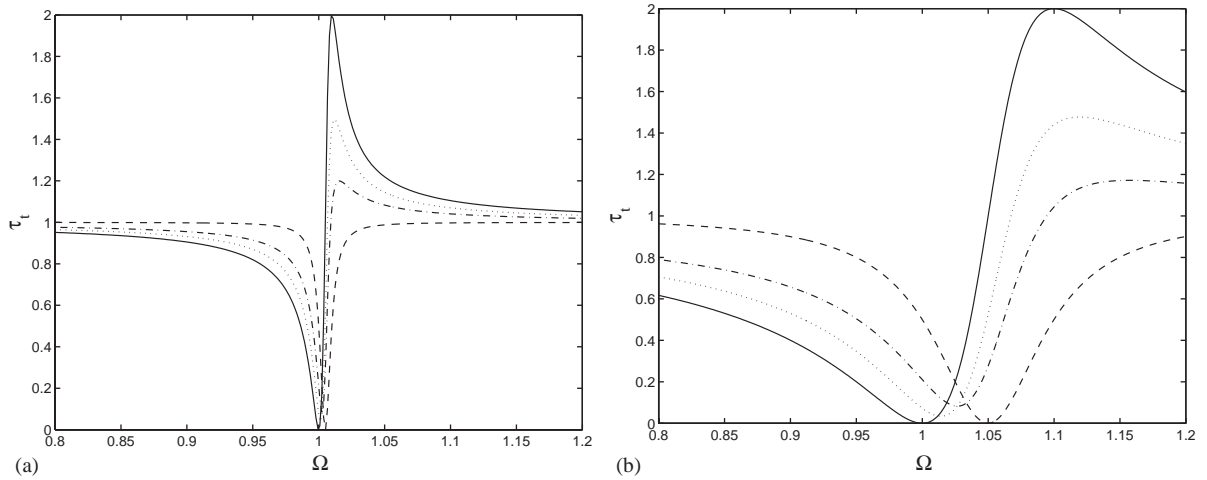


Fig. 2. The transmission ratio as a function of Ω for various l/λ_a , $\eta = 0$: (a) $\gamma = 0.01$; (b) $\gamma = 0.1$: — $l/\lambda_a = 0$; $l/\lambda_a = 0.05$; - · - · - $l/\lambda_a = 0.1$; - - - - $l/\lambda_a \gg 1$.

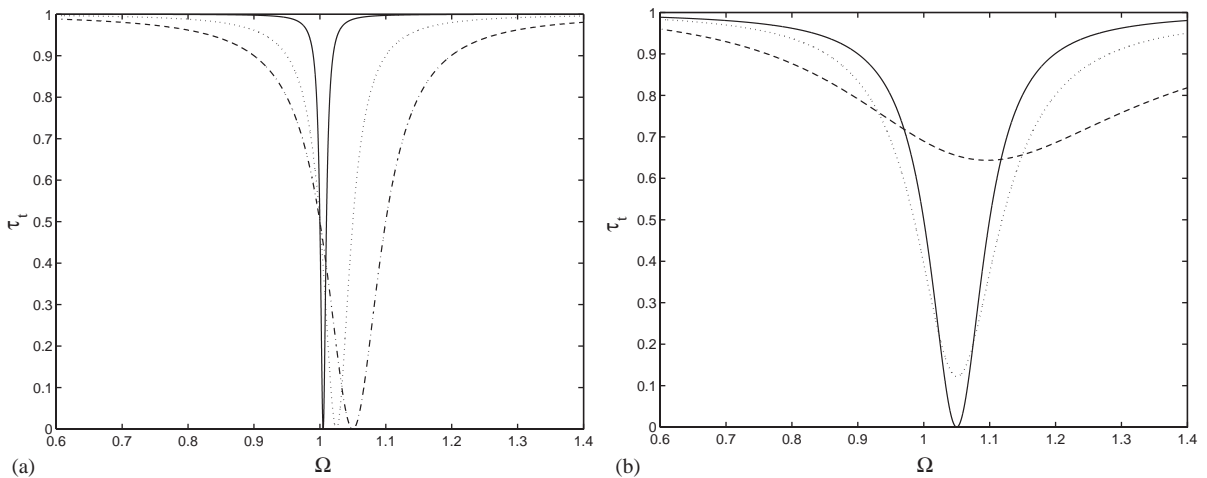


Fig. 3. Power transmission coefficient as function of Ω , TVA in the farfield: (a) undamped TVA: — $\gamma = 0.01$; $\gamma = 0.05$; - · - · - $\gamma = 0.1$; (b) damped TVA ($\gamma = 0.1$): — $\eta = 0$; $\eta = 0.05$; - · - · - $\eta = 0.1$.

3.2. TVA located in the farfield

If the TVA is positioned in the farfield of the point disturbance then evanescent waves incident on the TVA are negligibly small. The effect of the mass ratio on the power transmitted for an undamped TVA is shown in Fig. 3(a). Increasing the mass ratio increases the tuned frequency ratio Ω_t .

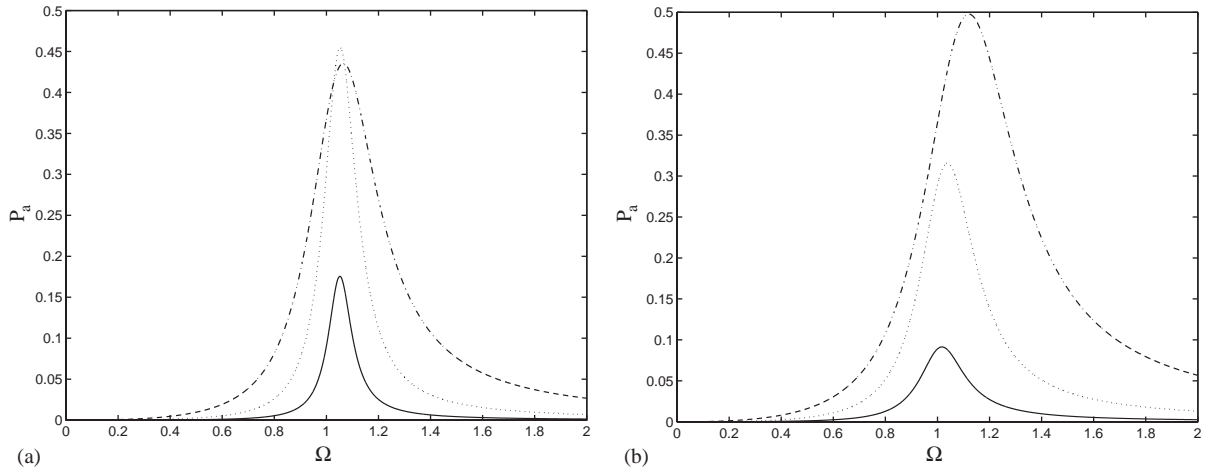


Fig. 4. The normalized power absorbed by the TVA as function of Ω , $l/\lambda_a \gg 1$. (a) $\gamma = 0.1$: — $\eta = 0.01$; $\eta = 0.05$; - - - - - $\eta = 0.2$. (b) $\eta = 0.2$: — $\gamma = 0.01$; $\gamma = 0.05$; - - - - - $\gamma = 0.2$.

Fig. 3(b) illustrates the effect of damping on the performance of the TVA. Although damping reduces the attenuation of the power transmitted at Ω_t , it also increases the proportion of the incident power absorbed by the TVA as shown in Fig. 4. Increasing the damping gradually increases the maximum power absorbed P_a (the power absorbed per input power) for a constant mass ratio until the damping reaches a particular limit. This is approximately when $\eta \approx \gamma$, as shown in Appendix A, when half of the incident power is absorbed, while the other half is equally transmitted and reflected. When $\eta > \gamma$, then the maximum power absorbed decreases as shown in Fig. 4(a), while the frequency Ω_b at which the maximum absorption occurs increases with η . The effect of γ on the proportion of incident power absorbed by the TVA is shown in Fig. 4(b). Increasing γ increases P_a as well as Ω_b for a fixed level of damping as long as $\gamma < \eta$. This latter effect is insignificant if the TVA is lightly damped. The maximum power that can be absorbed by the TVA cannot exceed half the incident power, since the beam is only restrained translationally, and the TVA cannot affect energy flow due to rotational (bending moment) components.

3.3. Optimum location of the TVA

The optimum location of the absorber at which the minimum power flows up- and downstream can be chosen by taking both τ_t and τ_r into consideration as shown in Fig. 5. The optimum location of the TVA is at one of the normalised distances (l/λ_a) that give the maximum attenuation of τ_r (approximately at multiples of $0.5\lambda_a$). The minimum values of τ_r and the value of τ_t for a farfield location depend on η , and tend to zero as $\eta \rightarrow 0$.

3.4. Optimum tuning

Fig. 6 shows the tuned frequency ratio Ω_t as a function of l/λ_a for various γ . Generally, Ω_t increases with $1/\lambda_a$ and asymptotes to the values given by Eqs. (23) and (25) when the TVA is in

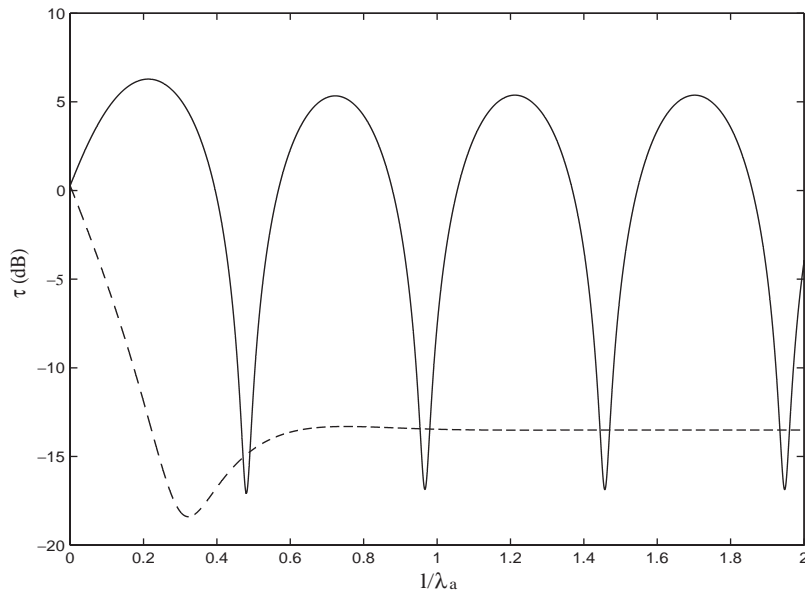


Fig. 5. Reflection and transmission ratios as function of normalized length at tuned frequency ratio $\Omega = 1.04$, $\gamma = 0.07$ and $\eta = 0.01$: — τ_r ; - - - τ_t .

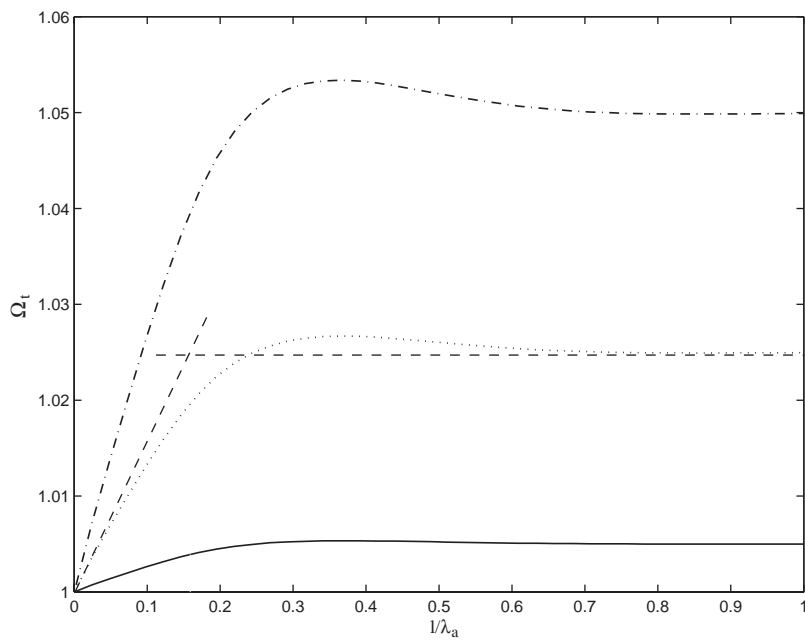


Fig. 6. Optimum tuning frequency as a function of l/λ_a , $\eta = 0$: — $\gamma = 0.01$; $\gamma = 0.05$; - - - $\gamma = 0.1$; - . - . - low and high l/λ_a asymptotes for $\gamma = 0.05$.

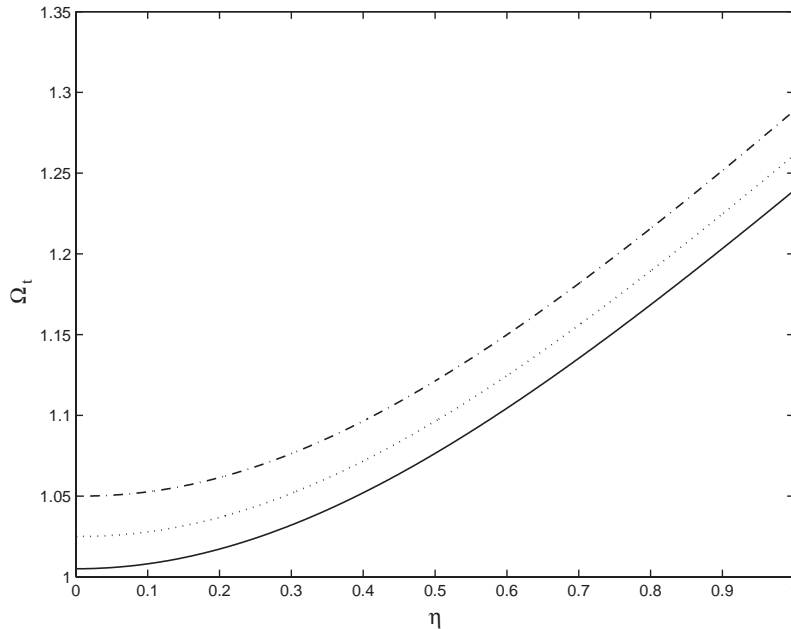


Fig. 7. The effect of damping on the tuned frequency ratio Ω_t , for an absorber located in the farfield: — $\gamma = 0.01$; $\gamma = 0.05$; - - - - - $\gamma = 0.1$.

the farfield and nearfield, respectively. These asymptotes are shown in Fig. 6 for $\gamma = 0.05$. Increasing the mass ratio increases Ω_t for a given location of the TVA. The minimum power transmitted generally occurs at higher tuned frequency ratios if the TVA is located further away from the point disturbance. This is not the case in the farfield, when the position of the TVA no longer affects Ω_t for a given γ . The tuned frequency is not affected by damping when $\eta \ll 1$. The effects of the mass ratio and the damping on Ω_b are similar to their effects on Ω_t . It is also worthy of note that Ω_b is greater than Ω_t .

The optimum tuning parameters of an absorber attached in the farfield can be found from Eqs. (17) and (20). Fig. 7 shows the relation between Ω_t and the damping of the absorber for various γ . Increasing η and/or γ increases Ω_t . A trade off should combine the beneficial effects of both η and γ for the best exploitation of the absorber, where increasing η would reduce the attenuation of the transmitted power.

The optimum parameters of the TVA at which the maximum power is absorbed are found numerically and are illustrated in Fig. 8. Designing a TVA with a higher value of structural damping than the optimum value indicated in Fig. 8 for a given mass ratio will reduce the maximum power absorbed by the TVA.

4. Experimental work

In this section, experimental measurements are compared with the theoretical and numerical predictions of Sections 2 and 3.

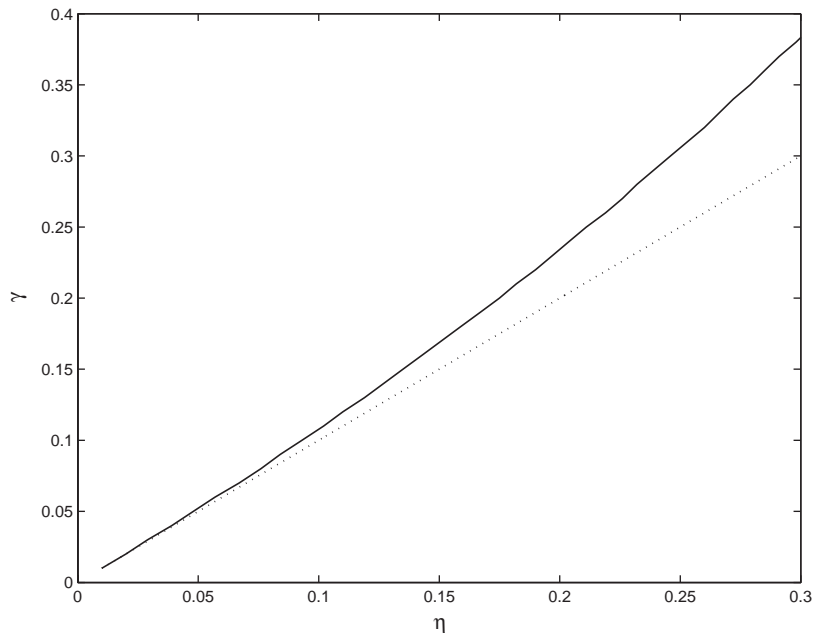


Fig. 8. Optimum parameters for maximum power absorption: — numerical prediction; numerical approximation ($\gamma = \eta$).

The absorber was made of a steel beam (1.7 mm × 20.5 mm × 80.4 mm) with blocks of brass (10.3 mm × 10.2 mm × 20 mm) attached at each end. The absorber was attached at its centre to a 6.4 mm × 50.6 mm × 5630 mm straight steel beam suspended at four points along its length. The ends of the beam were embedded in sand boxes to reduce reflections. The measured wavenumber of the beam was such that $k = 0.83\sqrt{f}$ where f is the frequency in Hz. The mass ratio of the TVA was predicted to be $\gamma = 0.07$ using Eq. (12a), thus the estimated masses were predicted to be $m_a = 45.7$ g while the mass that was effectively attached to the beam = 21.9 g. These values were obtained in a similar way to the model discussed by Hixson [10], while $f_a \approx 343$ Hz as described in Appendix B. The loss factor of the TVA was estimated to be $\eta = 0.0097$ using the circle fit method.

The beam was excited by a Ling V201 shaker with band-limited random noise over a frequency range 50–800 Hz. The propagating wave amplitudes were estimated using the frequency domain wave decomposition approach. This requires measuring the acceleration along the beam at four different points. Four PCB type 352C22 accelerometers were employed to measure the required accelerations. Other equipment included a spectrum analyser, power amplifier and a signal conditioner.

The accelerometers were divided into two pairs as shown in Fig. 9. The first pair (A_1 and A_2) was used to estimate the upstream propagating wave amplitude, while the second pair (A_3 and A_4) was used to estimate the downstream propagating wave amplitude. This allows measurement of wave amplitudes with or without the absorber attached to the beam, and hence estimation of the transmission and reflection ratios.

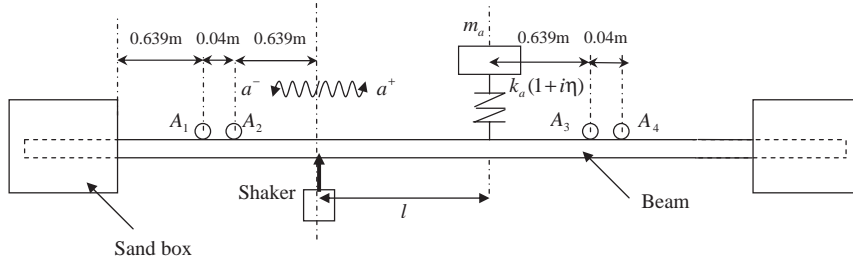


Fig. 9. Experimental set-up.

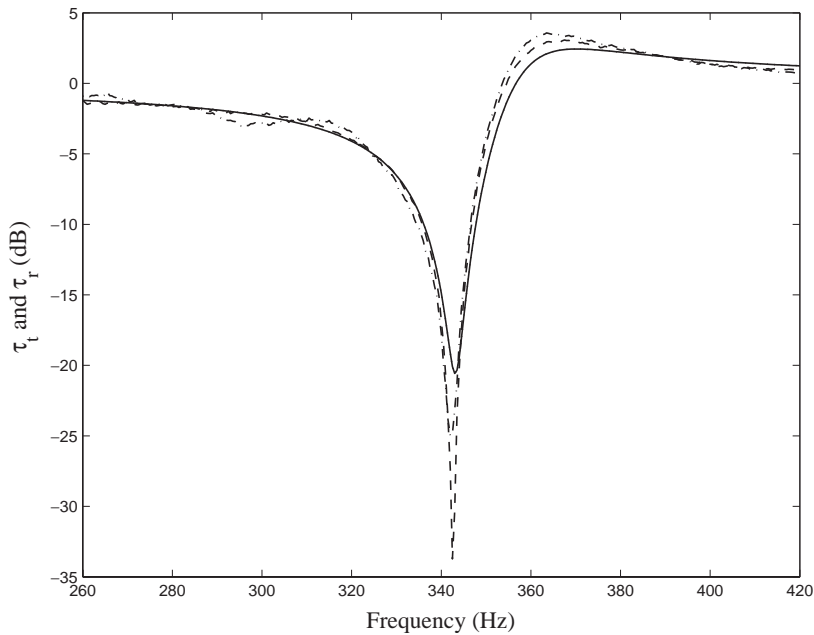


Fig. 10. Reflection and transmission ratios, $l/\lambda_a = 0$: — τ_r and τ_t theory; - - - - - τ_r , experiment; ······ τ_t , experiment.

The distance between the two accelerometers in each array was chosen to be 40 mm for signal conditioning purposes. In order to avoid the effects of nearfield waves above 150 Hz, the distance between each of the sand boxes, the absorber, the source of disturbance and the accelerometer arrays was chosen to be greater than a wavelength at 150 Hz (0.62 m). Nevertheless, the distance between the point disturbance and the TVA took one of five different values ($l/\lambda_a = 0, 0.34, 0.49, 0.73$ and 0.98 , where $\lambda_a = 0.41$ m) to examine the effects of the location of the TVA.

Fig. 10 compares the numerical predications of Eq. (16) to the experimental measurements when the TVA is attached to the point where the disturbance acts ($l/\lambda_a = 0$). For this case τ_r and τ_t should be equal. Control at the absorber frequency of 343 Hz can be clearly seen. The measured

powers transmitted downstream and upstream are nearly equal. Moreover, the tuned frequency is seen to be the same as the absorber frequency as predicted. The maximum attenuation achieved was approximately 34 dB in the upstream power and 25 dB in the transmitted power. These values are very sensitive to the level of damping in the TVA.

The effects of the location of the TVA were investigated experimentally by choosing four different locations of the TVA. Results are shown in Fig. 11. Agreement is generally good. A clear notch in τ_t is seen around the tuned frequency, while τ_r depends strongly on the location of the TVA. In Fig. 11(a) $l/\lambda_a = 0.34$, so that the TVA is well within the nearfield of the disturbance. However, in Fig. 11(b) $l/\lambda_a = 0.49$, so that there are still significant nearfield effects. Now there is also a clear notch in τ_r , due to the interference of the two wave components a^- and b^-e^{-ikt} . Locating the TVA at $l/\lambda_a = 0.73$ has increased the reflection ratio by approximately 5 dB as shown in Fig. 11(c). The tuned frequency here has slightly increased to 356 Hz. Fig. 11(d) shows the case where choosing an optimum location for the TVA achieves attenuation in both τ_t and τ_r . The tuned frequency here was found to be approximately 356 Hz as predicted.

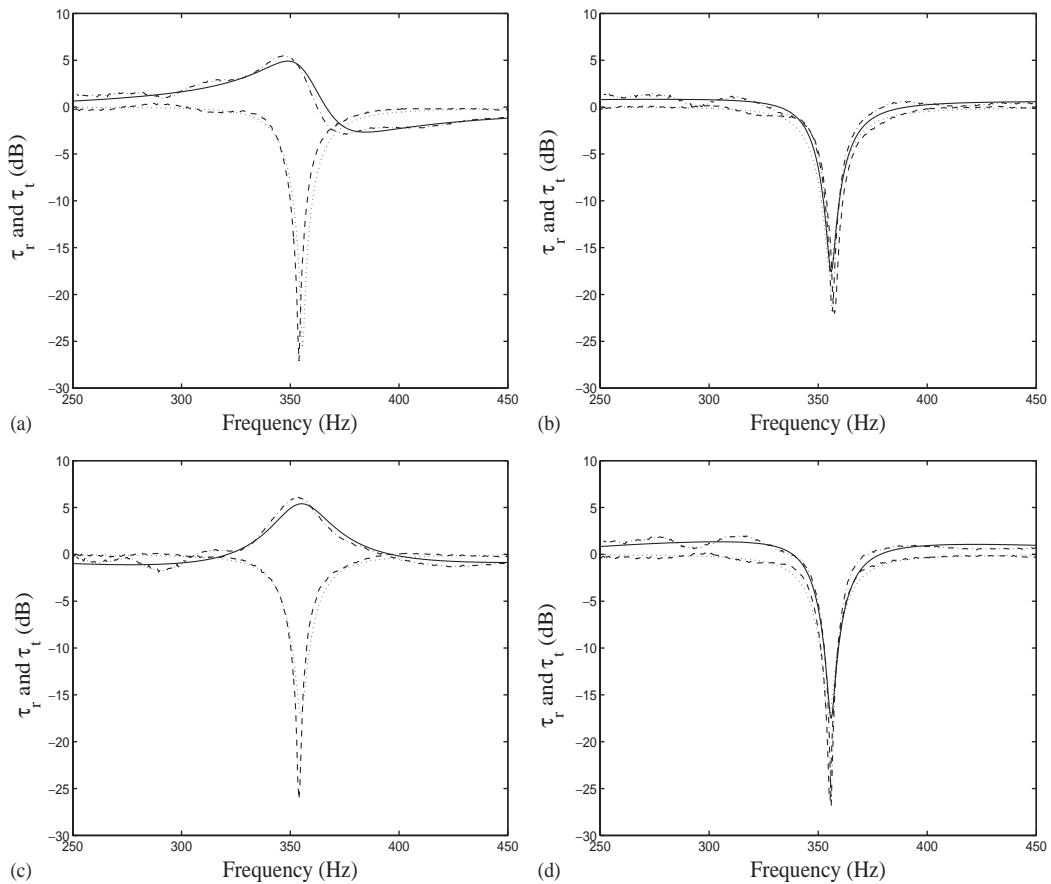


Fig. 11. Power reflection and transmission: (a) $l/\lambda_a = 0.34$; (b) $l/\lambda_a = 0.49$; (c) $l/\lambda_a = 0.73$; (d) $l/\lambda_a = 0.98$: — τ_r , theory; - - - τ_r , experiment; τ_t , theory; - · - · τ_t , experiment.

The disagreement at low and high frequencies is due to measurement errors and sensor miscalibration. Moreover, it is difficult to estimate the structural damping accurately which affects the response around the tuned frequency.

5. Conclusions

This paper has presented theoretical and experimental investigations of the behaviour and the optimum tuning parameters of a TVA, which suppresses flexural waves in thin beams. The location of the TVA with respect to a point disturbance has been taken into account.

The reflection and transmission ratios for the TVA were derived and depend on four independent tuning parameters: the absorber frequency ω_a , the mass ratio γ , the damping η , and the non-dimensional distance l/λ_a between the TVA and the disturbance. Emphasis was placed on finding the tuning parameters, which ensure the minimum power transmitted and reflected or the maximum power absorbed.

Analytical expressions for the transmitted and reflected powers were found to have components arising from both the propagating and evanescent waves. The location of the TVA only affects the tuned frequency if the incident evanescent waves are significant. In general, increasing the distance between the TVA and the source of disturbance would achieve the maximum attenuation in the transmitted power at a higher frequency ratio regardless of the power reflected upstream. Attenuation in the power flow in both directions can be achieved at the tuned frequency if the absorber is attached at certain distances from the point disturbance. These locations are approximately multiples of half the wavelength at the absorber frequency.

Numerical investigations have shown how increasing the mass ratio increases the tuned frequency and the frequency at which the maximum power is absorbed. Conversely, damping was found to reduce the attenuation of the transmitted power but it increases the tuned frequency.

Damping was also found to reduce the maximum transmission ratio, which occurs when the TVA is attached in the nearfield of a point disturbance. It was shown that the frequency at which the maximum power transmission occurs is greater than the tuned frequency. The theoretical predictions have been successfully validated by experimental measurements.

Acknowledgements

The authors would like to acknowledge the financial support provided by the Engineering and Physical Sciences Research Council (EPSRC).

Appendix A. Maximum power absorption by the absorber

An approximation for the optimum mass ratio, which achieves the maximum power absorption, can be attained by taking the impedance of the TVA and that of the beam into

consideration. The translational impedance of the beam is given by [1]

$$Z_{\text{beam}} = \frac{2EI k^3}{\omega} (1 + i). \tag{A.1}$$

The impedance of the TVA that ensures that it absorbs the maximum power is the complex conjugate of the impedance of the beam as stated in the “maximum-power-transfer theorem” [11] between two devices in a network, and is given by

$$Z_{\text{TVA}} = \frac{2EI k^3}{\omega} (1 - i) \tag{A.2}$$

The impedance of a TVA given by Brennan [3] can be reformulated using the parameters given in Eqs. (12a) and (12b) and written in non-dimensional form as

$$\frac{i\omega Z_{\text{TVA}}}{4EI k^3} = \frac{-\gamma \Omega^{1/2} (1 + i\eta)}{1 - \Omega^2 + i\eta}. \tag{A.3}$$

Assuming $\eta \ll 1$ then $\Omega_t^2 \approx 1 + \gamma \Omega_t^{1/2}$. Substituting this into Eq. (A.3) gives

$$\frac{i\omega Z_{\text{TVA}}}{4EI k^3} = \frac{-\gamma \Omega_t^{1/2} (1 + i\eta)}{-\gamma \Omega_t^{1/2} + i\eta}. \tag{A.4}$$

Assuming also $\gamma \ll 1$ and $\Omega_t \approx 1$, which are often the case in practice, then Eq. (A.2) can be substituted into Eq. (A.4) resulting in the relationship $\eta/\gamma \approx 1$. This means that for maximum power absorption by the TVA the loss factor should be approximately equal to the mass ratio.

Appendix B. Estimating the characteristics of the absorber

The absorber frequency and the resonance frequency of the beam-like absorber shown in Fig. 12(a) were estimated experimentally, as well as the structural damping and the absorber masses used in the model. At the absorber frequency, the motion at the attached point is small. The absorber was attached to a PCB impedance head-type 288D01 fitted to a Ling V201 shaker which excited the absorber with random noise in the frequency range 0–800 Hz. The impedance of the absorber in this frequency range, using a simple 2-dof system approximation shown in Fig. 12

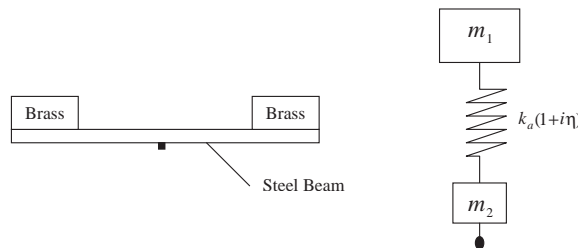


Fig. 12. Beam-like TVA.

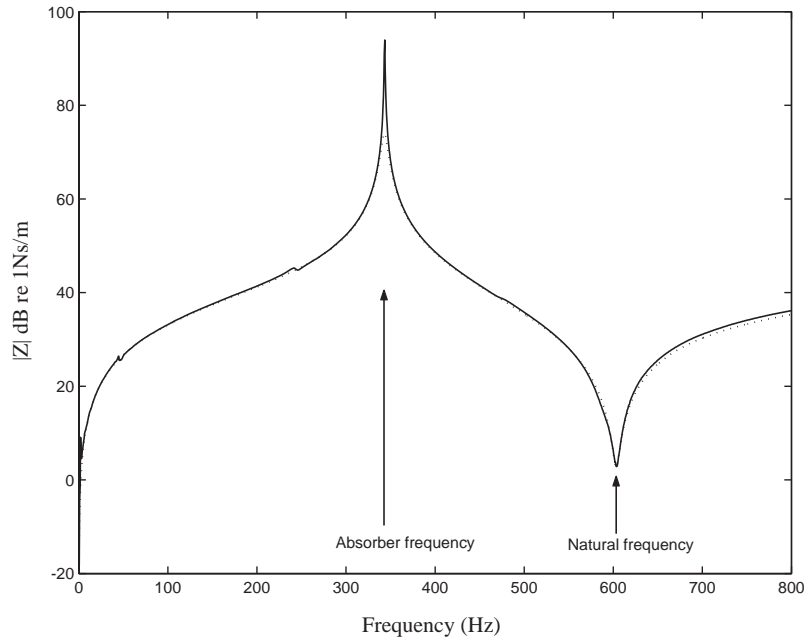


Fig. 13. Experimental and theoretical impedance of the absorber: — experimental; theoretical.

[10], is given by

$$Z = \frac{cm_1k_a\omega}{m_1k_a\omega - ick_a + icm_1\omega^2} + im_2\omega. \quad (\text{B.1})$$

The comparison between the theoretical and experimental point impedance of the absorber is shown in Fig. 13. It is clearly shown that the numerical prediction using Eq. (B.1) is very close to the experimental result. The modelled masses m_1 and m_2 of the absorber were estimated using knowledge of the experimental absorber frequency ($f_a = 343$ Hz) and resonance frequency ($f_r = 603$ Hz). Also $\omega_a = \sqrt{k_a/m_1}$ and $\omega_r = \sqrt{k_a(m_1 + m_2)/m_1m_2}$ [10]. The total mass of the absorber ($m_1 + m_2 = 67.6$ g) was found experimentally from the point acceleration at low frequencies. Therefore, $m_1 = 45.7$ g and $m_2 = 21.9$ g. The stiffness of the model was thus found to be $k_a = 212.6$ kN/m, while the damping constant was estimated to be $\eta = 0.008$ (best fit to experimental measurement).

References

- [1] D.J. Mead, Structural wave motion, in: R.G. White, J.G. Walker (Eds.), *Noise and Vibration*, Ellis Horwood, Chichester, 1982 (Chapter 9).
- [2] P. Clark, Devices for Reduction of Pipeline Vibration, Ph.D. Thesis, University of Southampton, 1995.
- [3] M.J. Brennan, Control of flexural waves on a beam using a tunable vibration neutralizer, *Journal of Sound and Vibration* 222 (1998) 389–407.

- [4] A.H. Von Flotow, A. Beard, D. Bailey, Adaptive tuned vibration absorbers: tuning laws, tracking agility, sizing, and physical implementations, *Proceedings of Noise-Con 94*, Fort Lauderdale, FL, USA, 1–4 May 1994, pp. 437–454.
- [5] K. Williams, G. Chiu, R. Bernhard, Geometric design of adaptive tuned vibration absorbers, *Proceedings of Inter-Noise 99*, Fort Lauderdale, FL, USA, 6–8 December 1999, pp. 901–906.
- [6] J.Q. Sun, M.R. Jolly, M.A. Norris, Passive, adaptive and active tuned vibration absorbers—a survey, *Transactions of the ASME* 117 (1995) 234–242.
- [7] R.J. Bernhard, H.R. Hall, J.D. Jones, Adaptive-passive vibration control, *Proceedings of Inter-Noise 92*, Toronto, Ont., Canada, 20–22 July 1992, pp. 427–430.
- [8] B.R. Mace, Wave reflection and transmission in beams, *Journal of Sound and Vibration* 97 (1984) 237–246.
- [9] L. Cremer, M. Heckl, E.E. Ungar, *Structure-Borne Sound*, second ed., Springer, Berlin, 1988.
- [10] E.L. Hixson, Mechanical impedance and mobility, in: C. Harris, C. Crede (Eds.), *Shock and Vibration Handbook*, McGraw-Hill, New York, 1976 (Chapter 10).
- [11] R.G. Meadows, Network theorems, equivalence and reduction, in: *Electric Network Analysis*, Penguin Education, Middle sex, 1972 (Chapter 6).